Sensitivity Optimization of Millimeter/Submillimeter MKID Camera Pixel Device Design

J. Schlaerth[*], S. Golwala[†], J. Zmuidzinas[†], A. Vayonakis[†], Js. Gao[**], N. Czakon[†], P. Day[‡], J. Glenn[*], M. Hollister[†], H. LeDuc[‡], P. Maloney[*], B. Mazin[§], H. Nguyen[‡], J. Sayers[‡] and J. Vaillancourt[†]

[*]*Center for Astrophysics and Space Astronomy, University of Colorado, 593 UCB, Boulder, CO 80309, USA*
[†]*California Institute of Technology, 1200 E. California Blvd., M/S: 367/17, Pasadena, CA 91125, USA*
[**]*National Institute of Standards and Technology, 325 Broadway, MS 817.03, Boulder, CO 80305, USA*
[‡]*NASA Jet Propulsion Laboratory, Pasadena, CA 91109, USA*
[§]*University of California, Santa Barbara, CA, 93106, USA*

Abstract.
We are using Microwave Kinetic Inductance Detectors in a sub/millimeter camera for the Caltech Submillimeter Observatory. These detectors are microwave resonators that rely on submillimeter and millimeter-wave photons to break Cooper pairs, changing the surface impedance. This changes the resonator frequency and quality factor, Q, and is measured by probe signals sent through a feedline coupled to the detectors. The camera will be divided into 16 independent readout tiles, each of which will fit 144 resonators at different frequencies into 360 MHz of bandwidth. We discuss the effect of readout power and single pixel frequency responsivity on the NEP of the detectors. Finally, we consider the mapping speeds of a full tile as a function of Q, which is controlled through the detector volume. A lower Q at fixed optical power implies greater responsivity, while a higher Q decreases the collision probability - the likelihood that any two resonators will have close enough resonant frequencies for crosstalk to be unacceptably high. We find the optimal design based on these constraints, and the corresponding mapping speeds expected at the telescope.

Keywords: Radio Telescopes and Instrumentation . Superconducting infrared, submillimeter and millimeter-wave detectors
PACS: 95.55.Jz, 85.25.Pb

INTRODUCTION

Microwave Kinetic Inductance Detectors have been demonstrated to have reached interesting levels of sensitivity for applications involving submillimeter and millimeter-wave astronomy [1, 2, 3, 4]. We will use these detectors, coupled to lithographed phased-array slot antennas, in a multicolor sub/millimeter camera at the Caltech Submillimeter Observatory [5]. The detectors are multiplexed by tuning their resonant frequencies to avoid overlap. Here we find the optimal parameters for single-pixel sensitivity, including the optimal readout power - the power in the signal sent in at the detector's resonance frequency to measure phase or amplitude change - and tuning of coupling to the readout feedline. We also discuss the tradeoffs faced between the sensitivity of the individual detectors and the total number of detectors, and find the optimal case for maximizing mapping speed.

SINGLE PIXEL SENSITIVITY CONSIDERATIONS

In normal operation, a probe signal is able to measure both the frequency shift and dissipation change of a resonator from an astronomical source. These are measured by detecting the change in amplitude and phase of a signal sent through the feedline at the resonance frequency, f_0. This change in transmission is given by

$$\delta S_{21} = \frac{Q^2}{Q_c}\left(\delta\frac{1}{Q_i} + i\frac{\delta f}{f_0}\right) \tag{1}$$

where Q_i is the internal Q without the contribution of coupling to the feedline, and Q_c is the Q for loss to the feedline. Higher order terms have been discarded.

Intrinsic responsivity

MKID detectors rely on incident radiation breaking Cooper pairs to change the surface impedance, leading to a measurable change in frequency and dissipation. If the quasiparticles follow a simple Fermi distribution of energies, we can quantify the intrinsic change by simply finding the number of quasiparticles created from the submillimeter light. Quasiparticle responsivity to an external power source with efficiency η is given by

$$\frac{dn_{qp}}{dP} = \left(\frac{\Delta^2 V^2}{\tau_0^2} + 4R\eta PV\Delta\right)^{-1/2} \tag{2}$$

where R is the quasiparticle recombination constant for the material, τ_0 is the unloaded lifetime, Δ is the gap parameter, and V is the resonator volume. The power source should be primarily submillimeter radiation coupled to the detector. However, the readout power at frequencies below the gap frequency has been shown to break Cooper pairs as well, though its efficiency is still under investigation.

The frequency shift per quasiparticle is related to this quasiparticle response by

$$\frac{df/f_0}{dP} = \frac{\alpha}{2} c(\Delta_0, T, f_0) \frac{dn_{qp}}{dP} \tag{3}$$

where $c(\Delta_0, T, f_0)$ is a function set for the resonator with no explicit dependence on P or n_{qp}, and α is the fraction of the resonator's inductance arising due to kinetic inductance, typically less than 10%.

In this mode of operation, frequency and dissipation responses are proportional, with the frequency response generally being a factor of several higher, determined from Mattis-Bardeen theory. Thus, any frequency response yields a proportional, though smaller, change in $1/Q_i$.

However, it has been demonstrated that MKIDs suffer two-level system noise in the frequency (phase) readout, but no such noise is apparent in the dissipation (amplitude) readout [2]. Thus, one is inclined to design for maximum quasiparticle responsivity in $1/Q_i$. In the presence of DC optical loading, an appreciable DC quasiparticle population is present. Therefore, increasing the quasiparticle responsivity thus also decreases the quiescent Q_i.

The only remaining device optimization is to ensure optimal coupling of the resonator to the feedline. The coupling is optimized when the coupling Q equals the internal Q, so that just as much power is dissipated in the resonator as is lost to the feedline. In reality, the dependence upon this optimization is weak, as a factor of two difference between the Qs only corresponds to an 11% drop in responsivity.

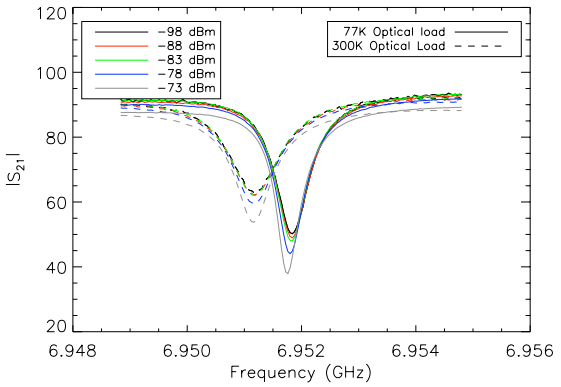

FIGURE 1. A plot of the transmitted feedline signal, S_{21}, as a function of frequency. The sweeps are taken while looking at 300K and 77K optical loads. One can see for both cases the power distortion of the resonance profile, and that Q increases with readout power. The powers shown are the readout powers estimated at the device.

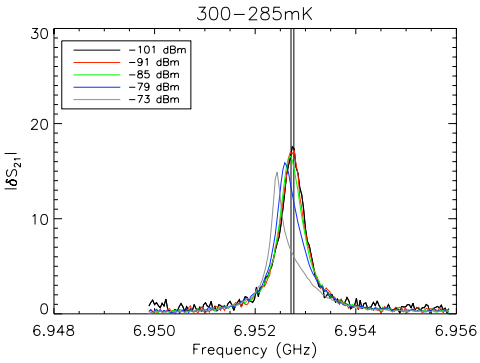

FIGURE 2. Here we show the magnitude change in the probe signal's S_{21}, in arbitrary units, due to a change in base temperature as a function of frequency. The vertical lines represent the resonant frequencies at the two base temperatures found at low power. As shown here, the high power detuning of the resonance frequency can be much greater than the effective frequency response. This shows that overall responsivity does not decline quickly with increased readout power.

Readout power dependence and noise

There are two primary non-astronomical noise sources: intrinsic detector noise [2, 3, 4] and amplifier noise. The intrinsic noise due to the substrate is caused by two-level system effects, and is seen as a frequency jitter. The amplitude of this noise, in squared fractional frequency shift per Hertz, goes down as $P^{-1/2}$, and amplifier noise decreases proportionally to the readout power. However, two factors must be taken into account. First, the readout power can create quasiparticles, though the efficiency is expected to be lower than for photons above the gap energy. Second, the resonance profile becomes distorted at high readout powers, likely due to a quasiparticle heating effect. As we gain in NEP with increasing power, the question becomes how much power can be applied before the NEP drops due to excess quasiparticle creation or to nonlinear or saturation behavior.

We can treat the readout power as an additional power term in Equation 2 with its own efficiency. Quasiparticle creation by readout power partially cancels the improvement in frequency jitter and readout noise. The optimum readout power depends on the value of this efficiency. If the efficiency is small, then there is no real limit to the noise reduction.

We have tested this by looking at frequency sweeps of the transmitted feedline signal over several resonators, both while looking at different optical loads and while varying the base temperature. These two methods are effectively equivalent [6]. From these data, we can make two inferences. First, at higher power, the resonance deepens, indicating an effectively higher Q likely due to quasiparticle heating, but it becomes more difficult to fit with a standard Lorentzian profile. This effect is seen in Figure 1. Second, the maximum responsivity is obtained by detuning from the low power resonance frequency (Figure 2). Although the resonance is distorted, and the optimal readout frequency changes with power, the overall responsivity does not change significantly. Further testing is required, but this leads to the possibility that much higher powers can be used to increase individual detector NEP.

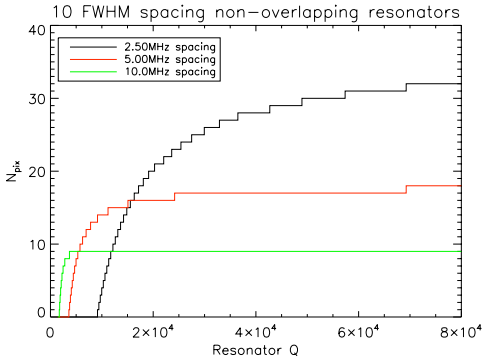

FIGURE 3. Number of detectors in each band which do not collide as a function of Q, at different nominal spacings. This assumes a 2MHz uncertainty between the predicted and actual frequency, and 90MHz bandwidth per color.

MAXIMIZING MAPPING SPEED

We have thus far considered single detector optimization. In practice, one must consider how to maximize not just NEP but also the mapping speed – the number of detectors multiplied by their beam solid angle, divided by the square of the NEP.

Because the resonators suffer some scatter in frequency about design values due to fabrication scatter, the chance of overlap among resonators is nonvanishing. Resonator overlap makes it difficult to disentangle the optical signals sensed by closely spaced resonators. In a fixed readout bandwidth (360 MHz in this case), the probability of overlap increases as the resonator Q_i decreases. Thus, while increasing responsivity improves individual detector NEP, doing so also decreases individual detector Q and makes resonator "collision," or crosstalk above a given threshold value, more likely. One must combine these two effects to find the optimal design Q, which is set primarily by the resonator volume.

We found the response in both frequency and Q_i to optical hot/cold loads, from which we can extrapolate the responsivity to any source power. We must also consider the efficiency of the readout power at breaking Cooper pairs, as this can affect Q_i. We then parameterize the sensitivity, the number of detectors likely to collide, and finally the mapping speed as a function of the expected Q. We then scale these values to what would be expected at resonant frequency at around 3.5GHz, the expected resonant frequency in the final MKID camera. We must consider several parameters in our calculation of mapping speed and optimization. Because the responsivity does not appear to degrade quickly with readout power, we assume that the pair-breaking efficiency of microwave readout power has a value of .10. The optimal readout power in this case is approximately 5dB higher than the expected optical loading. We take the scatter between resonators to be 2MHz RMS , which is in line with a recently designed device, and the resulting number of usable detectors is shown in Figure 3. At low Q, a larger spacing between resonators allows more detectors, but more can be fit in at high Q. We have run additional simulations with alternate values. These can change mapping speed values significantly; for example, a readout quasiparticle creation efficiency of unity reduces the sensitivity to below the background limited NEP expected at the telescope, and a lower scatter in resonance frequency increases the number of available detectors. However, the overall optimizations are relatively independent of specifics. We also consider different nominal resonator spacings, based on how many detectors we try to fit into the bandwidth.

We also assume several parameters in our models. The maximum crosstalk is set at the one percent of the maximum response of an adjacent resonator, beyond which we consider two resonators to have collided. We also assume optimal coupling, $Q_c = Q_i$. The cryogenic HEMT amplifier's noise temperature has been assumed to be 5K, and we assume the gain fluctuations will be easily removed as a common-mode signal.

The data combines noise data from submillimeter devices with noise data from new resonator designs not yet exposed to submillimeter power [7]. Finally, we assume a sky opacity model for photon noise and loading based on a model for Mauna Kea atmospheric conditions at an atmospheric opacity τ_{225GHz}=.106. The results given here are for a band detecting 200-260 GHz radiation, though the results are similar for other bands.

Given the assumptions, we can achieve background-limited performance under these conditions using dissipation readout, and near background limit in the frequency readout, as seen in Figure 4. This will not be true

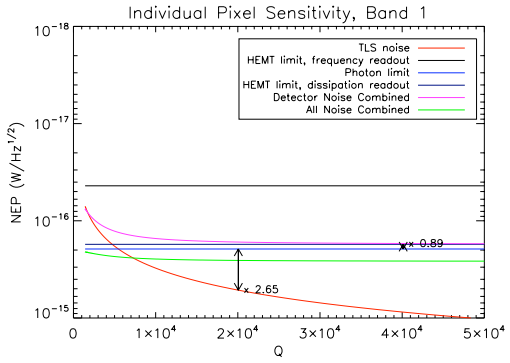

FIGURE 4. Here we see the NEP of the detectors as a function of Q. HEMT-limited dissipation readout is the best option at most Q values, while frequency readout requires low Qs to be competitive, limiting the number of detectors. At an intermediate Q of 20,000, frequency noise is already a factor of 2 above background-limited NEP.

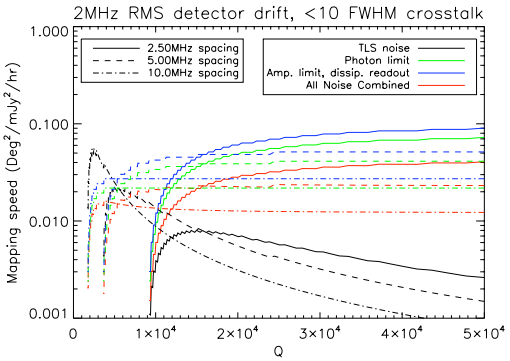

FIGURE 5. Mapping speed of the detectors as a function of Q. Here we see the different noise limitations. The optimal case involves using amplitude readout of large numbers of detectors, while frequency readout is hurt by excess frequency noise.

if we are not able to use as much readout power, as the noise is power dependent.

The optimal mapping speeds occur at relatively high Qs, which require large detector volumes and low intrinsic responsivity. The final signal is an optimal combination of both types of readout. As seen in Figure 5, the lower NEP dissipation readout will dominate in the circumstances of large numbers of detectors because the response is independent of Q. This fact is seen in Equation 1 – for an optimally coupled detector, any increase in $1/Q_i$ responsivity is canceled by a degradation in Q from a fixed load. Fundamental design and noise limitations, such as generation-recombination noise, prevent the use of very high Qs and corresponding low responsivity.

As is seen in Figure 4, to reach optimal NEP for individual detectors, one would have to significantly increase resonator spacing, and in the process reduce the mapping speed given a fixed bandwidth. When we also consider sky noise in excess of the nominal photon limit, it makes sense to incorporate a large number of detectors rather than a small number with optimized NEP.

CONCLUSIONS

Submillimeter MKID detectors have made great strides, and are now at the point where dissipation readout with high powers may approach background-limited sensitivity from the ground. Although there is a tradeoff between pixel sensitivity and the number of detectors, use of dissipation readout is in principle unaffected by these considerations. Therefore, designing detectors with lower responsivity in order to ensure a greater number of usable detectors is worthwhile to ensure maximum possible mapping speed. As readout bandwidth increases, the mapping speed will increase linearly, and such gains are to be expected in the future. While many facets require more explicit demonstration, such as the ability to remove amplifier gain variations and using high readout power to increase sensitivity, the potential sensitivities, and corresponding mapping speeds, appear promising for submillimeter astronomy applications.

ACKNOWLEDGMENTS

This research was funded by the National Science Foundation, grant AST-0705157 to the University of Colorado and California Institute of Technology, and personal support was given by the Graduate Student Researchers Program, grant 8743, through NASA/JPL. We would also like to acknowledge the contribution of the Gordon and Betty Moore Foundation, NASA ROSES support to the California Institute of Technology, and the JPL Research and Technology Development Fund.

REFERENCES

1. P. K. Day, H. G. LeDuc, B. A. Mazin, A. Vayonakis, and J. Zmuidzinas, *Nature* **425**, 817–821 (2003).
2. J. Gao, J. Zmuidzinas, B. A. Mazin, H. G. LeDuc, and P. K. Day, *Applied Physics Letters* **90**, 102507 (2007).
3. S. Kumar, J. Gao, J. Zmuidzinas, B. A. Mazin, H. G. LeDuc, and P. K. Day, *Applied Physics Letters* **92**, 128503 (2008).
4. J. Baselmans, S. Yates, R. Barends, J.-J. Lankwarden, J. Gao, H. Hoevers, and T. Klapwijk, *Journal of Low Temperature Physics* **151**, 524–529 (2008).
5. P. Maloney, *Journal of Low Temperature Physics* (2010).
6. J. Gao, J. Zmuidzinas, A. Vayonakis, P. Day, B. Mazin, and H. LeDuc, *Journal of Low Temperature Physics* **151**, 557–563 (2008).
7. O. Noroozian, *Journal of Low Temperature Physics* (2010).